ISSN 0020-1685, Inorganic Materials, 2006, Vol. 42, No. 10, pp. 1110–1114. © Pleiades Publishing, Inc., 2006.
Original Russian Text © D.O. Mishchuk, O.I. V'yunov, O.V. Ovchar, A.G. Belous, 2006, published in Neorganicheskie Materialy, 2006, Vol. 42, No. 10, pp. 1218–1222.

Synthesis and Dielectric Properties of $Sr_{0.6-x}Ba_{0.4}Na_{2x}Nb_2O_6$ Solid Solutions

D. O. Mishchuk, O. I. V'yunov, O. V. Ovchar, and A. G. Belous

Vernadsky Institute of General and Inorganic Chemistry, National Academy of Sciences of Ukraine, pr. Akademika Palladina 32/34, Kiev, 03680 Ukraine

e-mail: vyunov@ionc.kar.net

Received June 24, 2005; in final form, September 7, 2005

Abstract—We have prepared $Sr_{0.6-x}Ba_{0.4}Na_{2x}Nb_2O_6$ ($0 \le 2x \le 0.3$) solid solutions with the tetragonal tungsten bronze (TTB) structure, investigated the sequence of phase changes involved, and determined the lattice parameters of the solid solutions. The electrical properties of polycrystalline samples have been studied in broad frequency and temperature ranges. The results indicate that an increase in sodium content, accompanied by a reduction in the concentration of vacancies on the A site of the TTB structure, reduces the rate of dielectric relaxation.

DOI: 10.1134/S0020168506100116

INTRODUCTION

$Sr_yBa_{1-y}Nb_2O_6$ (SBN) solid solutions are relaxor ferroelectrics and are of considerable interest in designing pyroelectric sensors and electro-optic and piezoelectric devices [1, 2]. $Sr_yBa_{1-y}Nb_2O_6$ solid solutions exist in the composition range $0.2 \le y \le 0.8$ and have a so-called unfilled tetragonal tungsten bronze (TTB) structure [3, 4]. The unit cell of SBN can be represented by the general structural formula $[A(1)_2A(2)_4C_4][B(1)_2B(2)_8]O_{30}$, where A(1) stands for the 12-coordinate sites situated in tetragonal (in the *ab* plane) structural channels, A(2) stands for the 15-coordinate sites in pentagonal channels, and C represents the 9-coordinate sites in triangular channels (unoccupied in SBN). In the structure of SBN, the strontium and barium ions sit in two partially occupied sites, A(1) and A(2). The tetragonal sites A(1) are only occupied by strontium atoms, whereas the pentagonal sites A(2) are occupied by strontium and barium atoms at random. The disordering of the A atoms over two crystallographic sites is believed to be responsible for changes in the electrical properties of SBN, in particular for the relaxor behavior of its dielectric permittivity $\varepsilon(T)$ [5, 6]. Increasing the Sr : Ba atomic ratio reduces the phase-transition temperature of SBN, raises its dielectric permittivity, and makes its relaxor properties more pronounced, which shows up as a variation of the peak-permittivity temperature with frequency [7]. Note that, independent of the Sr : Ba ratio, one-sixth of the A sites in the structure of SBN are unoccupied. At the same time, the concentration and distribution of cation vacancies in the TTB structure may have a significant effect on the electrical properties of the material, as illustrated by the example of $Ba_{6-x}Ln_{8+2x/3}Ti_{18}O_{54}$ [8, 9].

The effect of cation vacancy concentration on the structure and electrical properties of SBN solid solutions has not been studied. Given that the synthesis of multicomponent oxide materials is typically a multistep process, it is reasonable to investigate the sequence of solid-state reactions underlying the formation of SBN with the aim of optimizing SBN synthesis.

In this paper, we report the synthesis, detailed structure, and electrical properties of SBN solid solutions in which the A vacancy concentration is varied through heterovalent substitution of sodium for strontium, as represented by the general formula $Sr_{0.6-x}Ba_{0.4}Na_{2x}Nb_2O_6$ ($0 \le 2x \le 0.3$).

EXPERIMENTAL

As starting chemicals, we used extrapure-grade Nb_2O_5, $BaCO_3$, $SrCO_3$, and Na_2CO_3. After calcination of Nb_2O_5 at 850°C, $BaCO_3$ and $SrCO_3$ at 400°C, and Na_2CO_3 at 200°C, appropriate amounts of the reagents were weighed out on a VLP-200 balance and then mixed and homogenized by grinding in a GKML-16 vibratory mill (agate vessels and chalcedony balls) under acetone. Thermal analysis was carried out in a MOM Q-1000 system. After synthesis at 1100–1200°C, the materials were reground in water, dried, and homogenized. Next, a plasticizer was added, and the powders were pressed into disks, which were then sintered between 1300 and 1350°C.

X-ray diffraction (XRD) measurements were made on a DRON-4-07 powder diffractometer (CuK_α radiation, 40 kV, 20 mA). Structural parameters were refined by the Rietveld profile analysis method. XRD patterns were collected in the angular range $2\theta = 10°$–$150°$ in

Crystal data for polycrystalline $Sr_{0.6-x}Ba_{0.4}Na_{2x}Nb_2O_6$ samples

Sample	$Sr_{0.6}Ba_{0.4}Nb_2O_6$ [11]	$Sr_{0.57}Ba_{0.4}Na_{0.006}Nb_2O_6$	$Sr_{0.55}Ba_{0.4}Na_{0.1}Nb_2O_6$	$Sr_{0.5}Ba_{0.4}Na_{0.2}Nb_2O_6$
Lattice parameters (sp. gr. *P4bm* (no. 100), *Z* = 10)				
a, Å	12.4566(9)	12.4521(2)	12.4489(2)	12.4417(2)
c, Å	7.8698(6)	7.8712(1)	7.8734(2)	7.8786(2)
V, Å	1221.1(2)	1220.47(3)	1220.18(4)	1219.57(4)
ρ_x, g/cm^3	5.286(1)	5.272(1)	5.262(2)	5.236(2)
Positional parameters				
Nb(1)(2*b*)*: *z*	0.00268(19)	0.005(4)	0.010(6)	0.010(5)
Nb(2)(8*d*): *x*	0.07451(3)	0.0741(1)	0.0736(2)	0.0750(2)
y	0.21161(3)	0.2115(1)	0.2115(2)	0.2111(2)
z	−0.00708(17)	−0.010(9)	−0.010(8)	−0.010(8)
Na/Sr(1)(2*a*)*: *z*	0.2382(2)	0.245(4)	0.240(4)	0.263(4)
Ba/Sr(2)(4*c*): *x*	0.17227(3)	0.1621(4)	0.1611(5)	0.1603(6)
y	0.67227(3)	0.6847(4)	0.6850(5)	0.6836(6)
z	0.24093	0.225(4)	0.251(8)	0.250(4)
O(1)(8*d*): *x*	0.2179(3)	0.2203(9)	0.226(1)	0.223(1)
y	0.2821(3)	0.2788(9)	0.273(1)	0.276(1)
z	−0.0150(15)	0.025(4)	0.055(4)	0.069(3)
O(2)(8*d*): *x*	0.1389(4)	0.139(1)	0.141(1)	0.151(3)
y	0.0695(3)	0.072(2)	0.070(2)	0.077(3)
z	−0.0254(11)	−0.025(5)	−0.025(5)	−0.010(5)
O(3)(2*b*): *x*	−0.0065(4)	−0.018(2)	−0.006(1)	−0.018(2)
y	0.3441(3)	0.336(3)	0.336(2)	0.348(3)
z	0.0229(14)	0.030(9)	0.025(9)	0.046(3)
O(4)(4*c*)*: *z*	0.2340(14)	0.236(4)	0.240(4)	0.240(3)
O(5)(8*d*): *x*	0.0838(9)	0.081(2)	0.093(2)	0.093(3)
y	0.2005(6)	0.204(2)	0.212(2)	0.221(2)
z	0.2299(9)	0.255(4)	0.256(4)	0.260(3)
Site occupancies				
Tetragonal channels (position 2*a*)				
Na	0.00	0.15	0.25	0.50
Sr(1)	0.71(5)	0.68(1)	0.67(1)	0.65(2)
Pentagonal channels (position 4*c*)				
Sr(2)	0.450(16)	0.41(1)	0.38(1)	0.30(1)
Ba	0.442(20)	0.487	0.487	0.487
Agreement factors				
R_B, %	3.3	7.05	9.59	9.90
R_f, %	4.5	6.52	8.03	9.11
Acentricity of Nb(1) and Nb(2) octahedra				
Δ[Nb(1)–O(4)], Å	0.29	0.30	0.31	0.31
Δ[Nb(2)–O(5)], Å	0.20	0.24	0.25	0.31

* Position 2*a*: 0, 0, *z*; 2*b*: 0, 1/2, *z*; 4*c*: *x*, 1/2 + *x*, *z*.

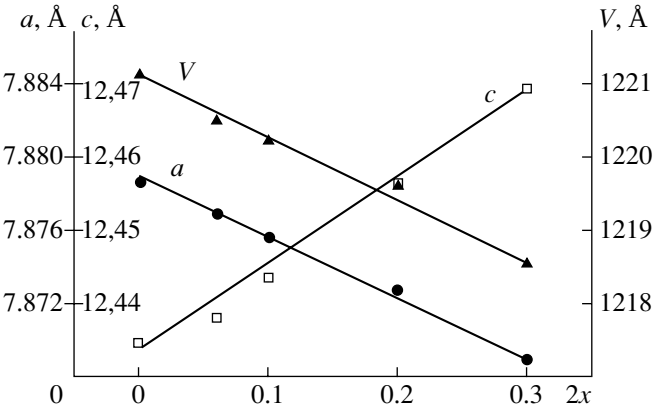

Fig. 1. Composition dependences of lattice parameters for $Sr_{0.6-x}Ba_{0.4}Na_{2x}Nb_2O_6$ solid solutions.

step-scan mode with a step size $\Delta 2\theta = 0.02°$ and a counting time of 10 s per data point. As external standards, we used SiO_2 (2θ calibration) and Al_2O_3 (NIST SRM1976 intensity standard [10]).

Dielectric permittivity, ε, and losses, $\tan\delta$, were measured in the range 10^5 to 10^6 Hz using a Tesla BM560 *Q*-meter and at 10^9 Hz using the coaxial line method. The samples were cylindrical in shape, 2 mm in diameter and 2 mm in height. Electrical contacts were made by firing silver paste.

RESULTS AND DISCUSSION

The phase changes involved in the synthesis of $Sr_{0.6-x}Ba_{0.4}Na_{2x}Nb_2O_6$ solid solutions via solid-state reactions were studied at $2x = 0.2$, which corresponds to the composition $Sr_{0.5}Ba_{0.4}Na_{0.2}Nb_2O_6$. According to XRD and thermal analysis data, the formation of this solid solution proceeds through the following intermediates: $NaNbO_3$, $Ba_5Nb_4O_{15}$, $Sr_5Nb_4O_{15}$, $BaNb_2O_6$, $SrNb_2O_6$, and $Ba_2NaNb_5O_{15}$. Based on these results, we optimized the synthesis procedure, using $NaNbO_3$, $BaNb_2O_6$, and $SrNb_2O_6$ as precursors.

Our data demonstrate that $Sr_{0.6-x}Ba_{0.4}Na_{2x}Nb_2O_6$ solid solutions with the TTB structure (sp. gr. *P*4*bm*) exist in a broad composition range. Increasing the sodium content to $2x \geq 0.3$, leads to the formation of Na_3NbO_4 as a second phase.

The structural parameters of polycrystalline $Sr_{0.6-x}Ba_{0.4}Na_{2x}Nb_2O_6$ samples are listed in the table. As input data, we used the positional parameters of the atoms in the structure of $Sr_{0.61}Ba_{0.39}Nb_2O_6$ [11].

The composition dependences of lattice parameters for $Sr_{0.6-x}Ba_{0.4}Na_{2x}Nb_2O_6$ solid solutions are displayed in Fig. 1. In the composition range studied, the lattice parameters are linear functions of sodium content, in line with Vegard's law. With increasing sodium content (decreasing strontium content), the *a* parameter decreases, while *c* increases.

At the same time, in the sodium-free system $Sr_{1-y}Ba_yNb_2O_6$, both *a* and *c* increase with decreasing strontium content [12]. The increase in *c* is caused by the elongation of the NbO_6 octahedra in the [001] direction, accompanied by Nb displacement from the center position of the oxygen octahedra and stronger acentricity of the octahedra [4]. The increase in *a* is due to the

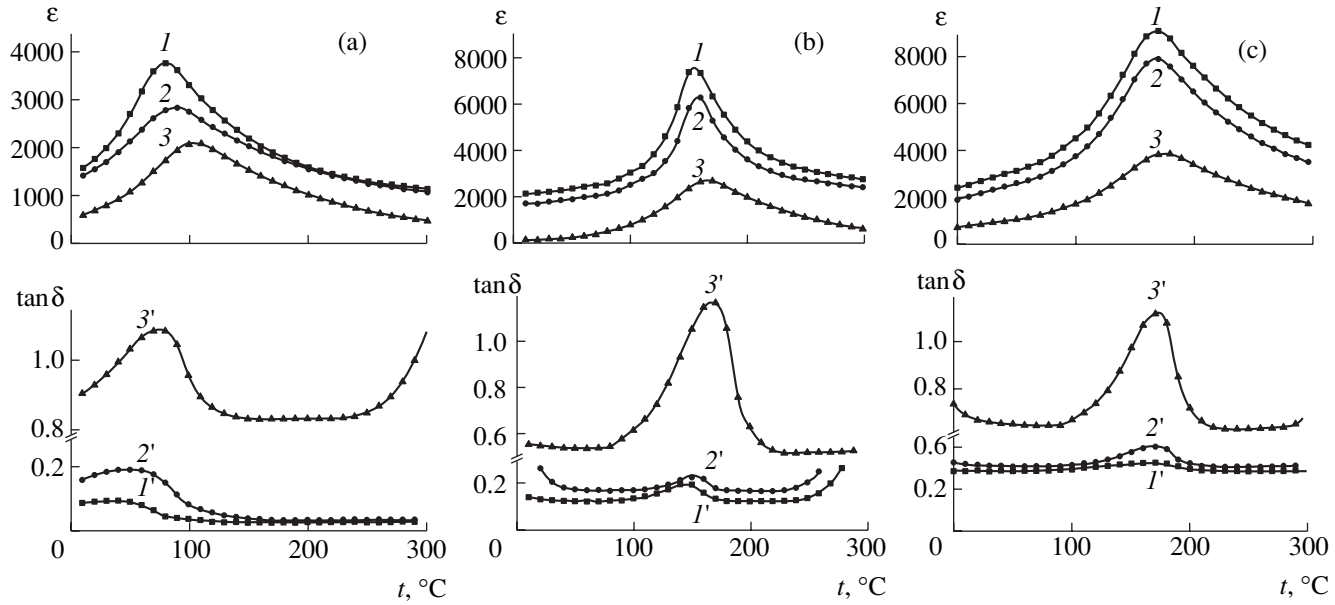

Fig. 2. Temperature dependences of (*1*–*3*) dielectric permittivity and (*1*'–*3*') losses for $Sr_{0.6-x}Ba_{0.4}Na_{2x}Nb_2O_6$ with $2x$ = (a) 0, (b) 0.1, and (c) 0.2 at (*1*, *1*') 10^5, (*2*, *2*') 10^6, and (*3*, *3*') 10^9 Hz.

increase in average ionic radius ($\bar{R} = \alpha R_{Sr} + \beta R_{Ba}$, where α and β are the mole fractions of strontium and barium, respectively) upon partial barium substitution for strontium in the pentagonal channels ($R_{Ba} > R_{Sr}$).

Increasing the sodium content of the $Sr_{0.6-x}Ba_{0.4}Na_{2x}Nb_2O_6$ solid solutions also increases the *c* parameter (Fig. 1) and the acentricity of the NbO_6 octahedra (table), but the *a* parameter decreases, which is attributable to the reduction in the average radius of the ions in the pentagonal channels because of the decrease in strontium occupancy in position 4*c* (table). It can be seen from the table that increasing the sodium content from $2x = 0$ to $2x = 0.2$ changes the site occupancies in the tetragonal and pentagonal channels: the occupancy of the twofold sites in the tetragonal channels increases from 0.71 to 1.15, whereas that of the fourfold sites in the pentagonal channels decreases from 0.89 to 0.79. The sodium atoms reside in the tetragonal channels, and the positive charge is compensated through the reduction in the amount of strontium in the pentagonal channels.

The dielectric properties of $Sr_{0.6-x}Ba_{0.4}Na_{2x}Nb_2O_6$ were studied at frequencies from 10^5 to 10^9 Hz. As can be seen from Fig. 2, the Na-free material ($x = 0$) is characterized by significant permittivity relaxation. In the frequency range studied, the maximum in ε shifts by 30°C. With an increase in sodium content, accompanied by a reduction in A vacancy concentration, the shift in $\varepsilon_{max}(t)$ (Δt_{max}) decreases (Fig. 3). This suggests that the A vacancy concentration in $Sr_{1-y}Ba_yNb_2O_6$ solid solutions with the TTB structure has a significant effect on their electrical properties. The present results demonstrate that reducing the cation vacancy concentration reduces the rate of dielectric relaxation.

The shift in peak-permittivity temperature T_{max} with increasing frequency can be analyzed using an Arrhenius-type equation [13],

$$f = f_0 \exp\left[\frac{-E_a}{kT_{max}}\right],$$

where *f* is the measurement frequency, $f_0 \approx 10^{13}$ Hz is the attempt frequency for ionic lattice vibrations [14], E_a is the activation energy of permittivity relaxation, T_{max} is the peak-permittivity temperature, and *k* is the Boltzmann constant. Figure 4 shows the plot of the logarithm of measurement frequency versus inverse peak-permittivity temperature. From the slope of this plot, one can evaluate the activation energy. Our results indicate that the activation energy in $Sr_{0.6-x}Ba_{0.4}Na_{2x}Nb_2O_6$ increases with sodium content, from $E_a = 3.00(8)$ eV at $2x = 0$ to $E_a = 6.04(3)$ eV at $2x = 0.1$. In the $2x = 0.2$ sample, there is no relaxation, which corresponds to an infinite activation energy.

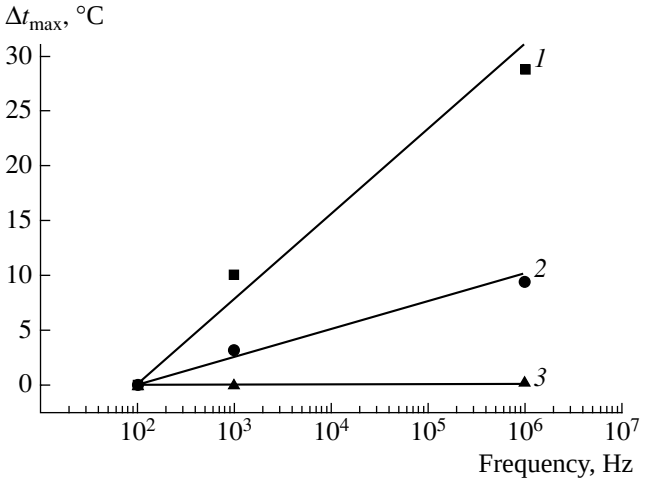

Fig. 3. Shift in peak-permittivity temperature as a function of frequency for $Sr_{0.6-x}Ba_{0.4}Na_{2x}Nb_2O_6$ with $2x$ = (*1*) 0, (*2*) 0.1, and (*3*) 0.2.

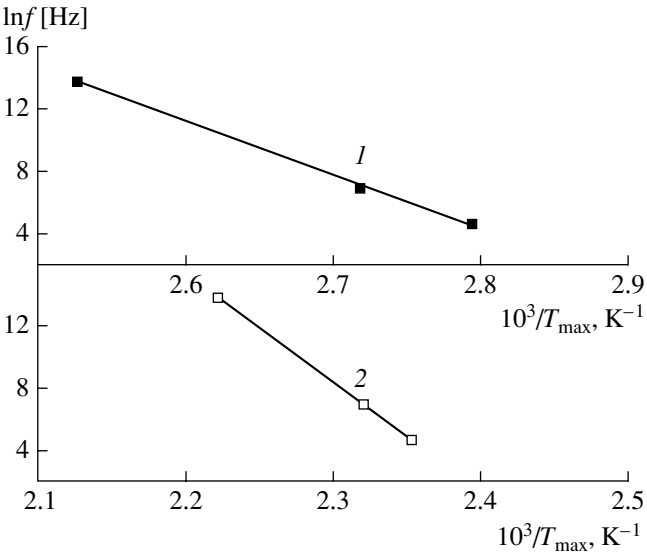

Fig. 4. Arrhenius plot of measurement frequency for $Sr_{0.6-x}Ba_{0.4}Na_{2x}Nb_2O_6$ with $2x$ = (*1*) 0 and (*2*) 0.1.

CONCLUSIONS

The present results demonstrate that the formation of $Sr_{0.6-x}Ba_{0.4}Na_{2x}Nb_2O_6$ solid solutions is a multistep process, involving $NaNbO_3$, $Ba_5Nb_4O_{15}$, $Sr_5Nb_4O_{15}$, $BaNb_2O_6$, $SrNb_2O_6$, and $Ba_2NaNb_5O_{15}$ as intermediates. Heterovalent substitution of sodium for strontium, accompanied by a reduction in A vacancy concentration, leads to linear variations in lattice parameters over the entire composition range studied, $0 \le 2x \le 0.3$, and reduces the rate of dielectric relaxation.

REFERENCES

1. Glass, A.M., Investigation of the Electrical Properties of $Sr_{1-x}Ba_xNb_2O_6$ with Special Reference to Pyroelectric Detection, *J. Appl. Phys.*, 1969, vol. 40, pp. 4600–4716.
2. Xu, Y., Li, Z., Wang, H., and Chen, H., Phase Transition of Some Ferroelectric Niobate Crystals with Tungsten-Bronze Structure at Low Temperature, *Phys. Rev. B: Condens. Matter Mater. Phys.*, 1989, vol. 40, pp. 11902–11908.
3. Myoung-Sup Kim, Peng Wang, Joon-Hyung Lee, et al., Site Occupancy and Dielectric Characteristics of Strontium Barium Niobate Ceramics: Sr/Ba Ratio Dependence, *Jpn. J. Appl. Phys., Part 1*, 2002, vol. 41, no. 11B, pp. 7042–7047.
4. Chernaya, T.S., Maksimov, B.A., Volk, T.R., et al., Atomic Structure of Single-Crystal $Sr_{0.75}Ba_{0.25}Nb_2O_6$ and Structure–Property Relations in (Sr,Ba)Nb_2O_6 Solid Solutions, *Fiz. Tverd. Tela* (S.-Peterburg), 2000, vol. 42, no. 9, pp. 1668–1672.
5. Cross, L.E., Relaxor Ferroelectrics, *Ferroelectrics*, 1987, vol. 76, pp. 241–267.
6. Oliver, J.R., Neurgaonkar, R.R., and Cross, L.E., A Thermodynamic Phenomenology for Ferroelectric Tungsten Bronze $Sr_{0.6}Ba_{0.4}Nb_2O_6$ (SBN:60), *J. Appl. Phys.*, 1988, vol. 64, no. 1, pp. 37–47.
7. Carrio, J.G., Mascarenhas, Y.P., Yelon, W., et al., Structure Refinement of (Sr,Ba)Nb_2O_6 Ceramic Powder from Neutron and X-rays Diffraction Data, *Mater. Res.*, 2002, vol. 5, no. 1, pp. 57–62.
8. Ohsato, H., Mizuta, M., Ikoma, T., et al., Microwave Dielectric Properties of Tungsten Bronze-Type $Ba_{6-3x}Nb_{8+2x/3}Ti_{18}O_{54}$ (R = La, Pr, Nb, and Sm) Solid Solutions, *J. Ceram. Soc. Jpn.*, 1998, vol. 106, no. 2, pp. 178–182.
9. Belous, A., Ovchar, O., Valant, M., et al., The Effect of Partial Isovalent Substitution in the A-Sublattice on MW Properties of Materials Based on $Ba_{6-x}Ln_{8+2x/3}Ti_{18}O_{54}$ Solid Solutions, *J. Eur. Ceram. Soc.*, 2001, vol. 21, pp. 2723–2730.
10. *Certificate of Analysis: Standard Reference Material 1976, Instrument Sensitivity Standard for X-ray Powder Diffraction*, Gaithersburg: National Inst. of Standards and Technology, 1991, p. 4.
11. Woike, T., Petříček, V., Dušek, M., et al., The Modulated Structure of $Ba_{0.39}Sr_{0.61}Nb_2O_6$: I. Harmonic Solution, *Acta Crystallogr., Sect. B: Struct. Sci.*, 2003, vol. 59, pp. 28–35.
12. Nikasch, Ch. and Göbbels, M., Phase Relations and Lattice Parameters in the System SrO–BaO–Nb_2O_5 Focusing on SBN ($Sr_xBa_{1-x}Nb_2O_6$), *J. Cryst. Growth*, 2004, vol. 269, pp. 324–332.
13. Do-Kyun Kwon, Randall, C.A., Shrout, T.R., and Langan, M.T., Dielectric Properties and Relaxation in $(1-x)BiScO_3$–$xBa(Mg_{1/3}Nb_{2/3})O_3$ Solid Solutions, *J. Am. Ceram. Soc.*, 2004, vol. 87, no. 6, pp. 1088–1092.
14. Cann, D.P., Randall, C.A., and Shrout, R.T., Investigation of the Dielectric Properties of Bismuth Pyrochlores, *Solid State Commun.*, 1996, vol. 100, no. 7, pp. 529–534.